for EMR retrieval for clinical research [11,22–25]. To ensure that the data retrieval process is practical and independent from the structure of the EMR system, a data warehouse (DWH) was created by extracting, transforming, and loading information from the EMR system. To retrieve and report information from multiple patients efficiently, an online analytical processing (OLAP) tool was installed [26]. The OLAP tool runs from an Internet browser and has the ability, in hypertext markup language (HTML), to report on information retrieved from the browser. The reports are created in various formats, such as PDF, CSV, and extensible markup language (XML). The ERS also was applied to the data recorded using the new template. We created reports for checking trial data and extracting data for statistical analysis.

Application to a clinical trial

We applied the system to a single-institution phase II trial for hepatocellular carcinoma. ('A randomised controlled study of effectiveness between transcatheter arterial chemoembolisation (TACE) with cisplatin and TACE with epirubicin for multiple hepatocellular carcinomas'). This study was approved by the ethics committee of Kyoto University Hospital and was registered in the UMIN Clinical Trials Registry [27] (registration number UMIN000003162).

Based on the findings from an observational study in our hospital [28,29], this phase II trial was designed to confirm the effectiveness of TACE in combination with one of the two anticancer agents. A total of 160 subjects will be enrolled, treated by a single TACE therapy, and evaluated for 12 months. Including laboratory tests, the number of data items per subject is approximately 80, and the number of total records per subject is approximately 15 (Table 1).

Procedures of the clinical trial

Preparation

In the pilot test of our clinical trial process model, we prepared seven templates: eligibility criteria, target lesion, protocol treatment, efficacy of treatment based on the European Association for the Study of the Liver (EASL) standard [30], efficacy of treatment based on the Response Evaluation Criteria in Cancer of the Liver (RECICL) standard [31], adverse events based on CTCAE 4.0, and follow-up (Table 1). Codes and grades (i.e., EASL, RECICL, CTCAE) were assigned by the investigators when they entered these data into the EMR using the clinical trial templates. Three types of ERS reports were used to check the clinical trial data: a list of cases, each patient's case registration form, and the CRF (Table 1). We show an example of the EMR template and progress notes from the EMR in Figure 2.

For the local data manager to verify the completeness and consistency of trial data, the CRF can

Table 1. The screen to record data for EMRs and the data check screen

Screen to record data for EMRs		Edit check screen
Template name	Item name	
Eligibility criteria	Informed consent	List of cases
	Registration number	Case registration form
	Date of consent	
	Result of allocation	
	Selection criteria 1–8	
	Exclusion criteria 1–10	
Target lesion	Number	Case report form
	Tumour location	
	Size (maximum)	
	Incipient TACE/ non-incipient TACE	
	Vascular invasion	
	Frequency of TACE	
Protocol treatment	Date of protocol treatment	
	Size (maximum)	
	Total dose	
	Number	
	Total dose for TACE	
	Tumour location	
	Addition of RFA/PEIT	
	Anticancer drug	
	Infusional therapy	
Efficacy of treatment (EASL); efficacy of treatment (RECICL)	Efficacy of treatment	
	Recurrence form	
	Plan of treatment	
	Other	
Adverse event	Abdominal pain	
	Cause of abdominal pain	
	Diarrhoea	
	Cause of diarrhoea	
	Nausea	
	Cause of nausea	
	Vomiting	
	Cause of vomiting	
	Fever	
	Cause of fever	
	Performance status	
	Other	
Follow-up	Date of progressive disease	
	Recurrence form	
	Treatment after recurrence	
	Conform to protocol treatment	
	Reason of change	
	Date of death	

EMR: electronic medical record; TACE: transcatheter arterial chemoembolisation; RFA: radiofrequency ablation; PEIT: percutaneous ethanol injection therapy; EASL: European Association for the Study of the Liver; RECICL: Response Evaluation Criteria in Cancer of the Liver.

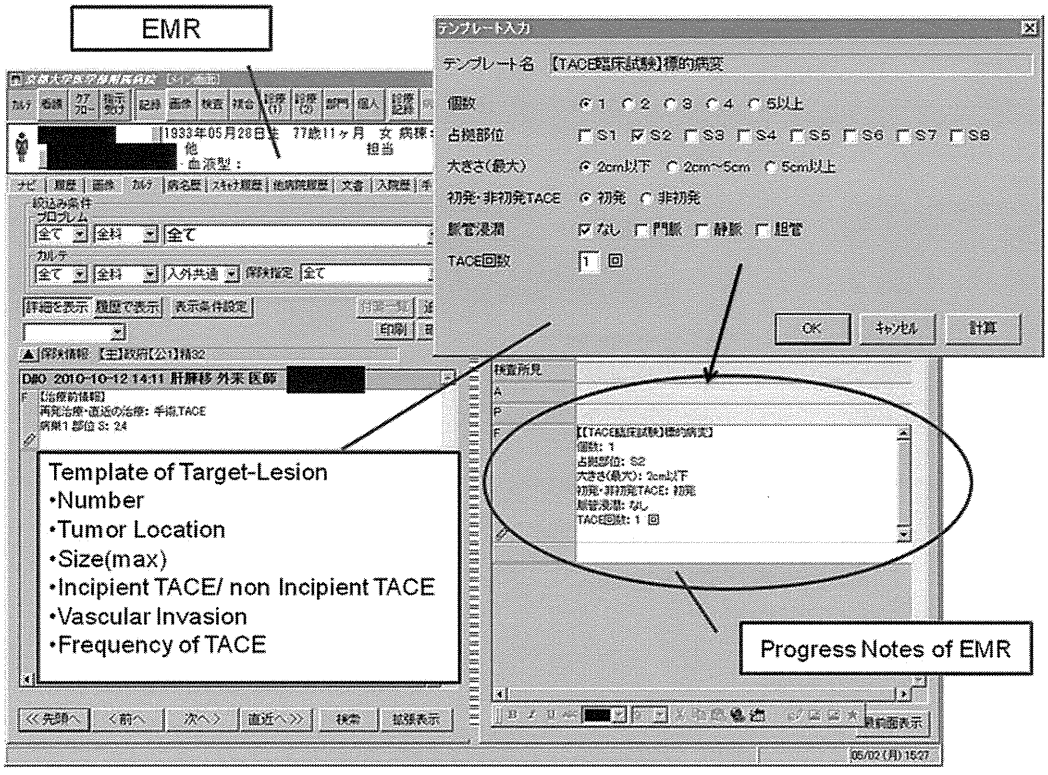

Figure 2. Electronic medical record (EMR) and the EMR template. The template is opened from within our EMR system. The template converts narrative information from progress notes, thereby making the information available as analytical data.
TACE: transcatheter arterial chemoembolisation.

be identified. The CRF summarises all the templates on one screen such that the integrity of all information for each patient can be assessed at a glance. The latest data for eligibility criteria, target lesion, protocol treatment, efficacy of treatment, and follow-up are displayed by item; adverse events are shown in sequence according to the name of the adverse event so that changes in the adverse event grade can be observed (Figure 3).

Patient registration and random assignment of treatment arm

Patients were registered and assigned randomly to a treatment arm in an independent registration centre outside of the EMR system. The investigator received the registration and assignment information and recorded it on the eligibility criteria template in the EMRs.

Recording clinical trial data in EMRs

The investigator conducted the protocol treatment and evaluations according to the clinical pathways and recorded the results in templates. The results of required laboratory tests were extracted directly from the EMRs.

Correction of data

Clinical trials often require local-level administrative help with the increased workload [4,32], but our model provides the local data manager with new responsibilities to ensure trial data quality. In the pilot study, a local data manager – a clinician at the participating site – manually checked the trial data for completeness and consistency using the CRF on the ERS. When the local data manager found incomplete or inconsistent trial data, he asked the investigator to determine whether data should be corrected. The investigator added necessary data using the original EMR templates, thus storing a revision history in the EMRs.

In the pilot study, the data in the EMR system create the edit checks and format the data for statistical analysis; thus, a separate EDC system or the CDMS is unnecessary. We executed data checks manually to ensure that the latest medical records were correct.

Extracting data for statistical analysis

We used the ERS to extract data for the statistical analyses according to predefined data formatting and coding conventions. After the data were presented for statistical analysis in the CSV by the ERS, reports of all

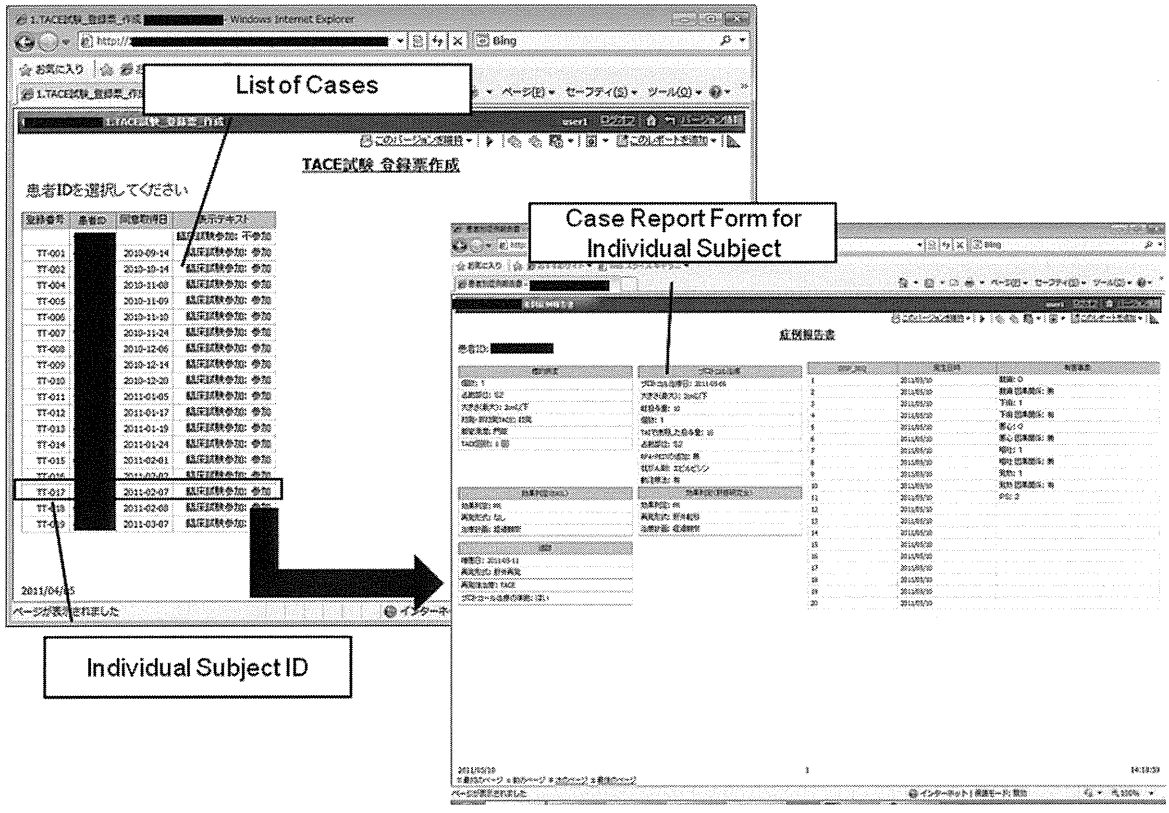

Figure 3. The list of cases and the CRF. The CRF can be consulted from the list of case registration forms. The CRF summarises all the templates on one screen, so that all information can be assessed at a glance.
CRF: case report form; TACE: transcatheter arterial chemoembolisation; EASL: European Association for the Study of the Liver; EMR: electronic medical record; RECICL: Response Evaluation Criteria in Cancer of the Liver.

the data were prepared and archived in PDFs with an electronic signature added to prevent manipulation.

Results

We applied our new system to an actual clinical trial and evaluated its feasibility. Using the list of registered patients in the registration centre, we determined whether we could extract both the data by templates and the laboratory results of the registered patients in pre-designed forms. We verified that the data could be extracted correctly and found no unexpected problems.

Regarding the clinical staff workload, the investigators did not need to complete CRFs or enter data into an EDC system in addition to the EMRs. Among the prepared templates for the clinical trial, the only one that was added to the pilot study was eligibility criteria for patient registration. The investigators had to record information in the medical records for TACE, including the number of tumours, their diameter and extent of vascular invasion, and the therapeutic regimen, such as anticancer drug doses and embolised arteries in the liver. To record the necessary clinical information on a patient's EMR, investigators used the templates based on the clinical pathways for TACE, and they checked the results of laboratory tests shown in the EMRs.

Regarding the data quality control, as the data in the EMR templates were identical to those in the ERS, the use of the EDC system or the CDMS was also unnecessary. When investigators added information to EMRs, local data managers viewed reports in the CRF automatically on the ERS. Local data managers check the data until all the errors are corrected. In this way, the progress of the clinical trial and the situation for each patient could be assessed at a glance.

Figure 4 shows the procedural differences among a paper-based clinical trial, a clinical trial using the EDC system, and our new model. In contrast with conventional clinical trials, our model made it unnecessary to transcribe data from medical records to CRFs, to execute source data verification (SDV) at the participating site, to transport paper-based CRFs from the participating site to the coordinating centre, or to make double entries in the CDMS from paper-based CRFs. In addition, data checking was performed by

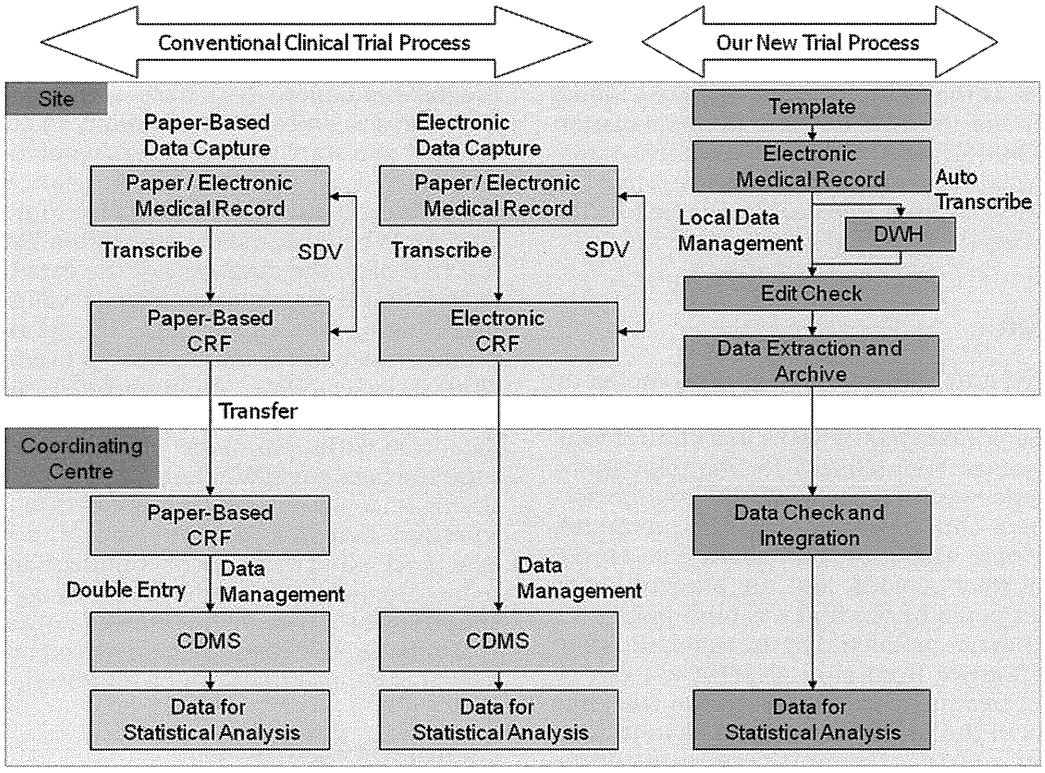

Figure 4. The pilot study revealed many advantages over a conventional clinical trial process, that is, unnecessary to transfer information from medical records to the CRF, no need for source data verification at the participating site, unnecessary to transmit the CRF from the participating site to the coordinating centre, and unnecessary to re-enter data into the CDMS from the paper-based CRF. In addition, data management in the coordinating centre was replaced with edit checks initiated by a local data manager at the participating site.
SDV: source data verification; CRF: case report form; DWH: data warehouse; CDMS: clinical data management system.

the local data manager at the participating site, and supplemental data checking and data integration were performed at the central coordinating centre.

Limitations

To execute clinical trials according to our model, specialised data must be accumulated from EMRs according to each clinical trial protocol. From a technical viewpoint, equipment for the flexible input functions, such as the EMR template, and efficient ERSs are required. Consequently, trials must be planned from the stage of protocol development. The pilot test trial was planned to answer the practical questions that clinicians face in clinical practice. If a clinical trial is not practice-based [33–35], then it will not be easy to add medical records using a template. In our model, the coordinating centre workload for data management and quality monitoring would be reduced. Instead, the workload of the local data manager at the participating site would be increased. In addition, in the test trial, every time errors were found in trial data using the CRF on the ERS, the local data manager had to communicate with the investigator. In the future, more efficient local data management methods will have to be established [36].

Because the test trial used for the pilot study was executed in a single institution, it was not necessary to integrate the clinical trial data from multiple participating sites. We used the CSV format to present data for statistical analysis and the PDF format to archive the trial data at the participating site. To execute multi-institutional clinical trials, it will be necessary to standardise the descriptions in EMRs, use evidence-based clinical pathways, and create and validate templates across EMRs at all participating sites [37]. Currently, the accuracy of the information in EMRs may vary across sites [12]. For example, there are standard medical terminologies, such as International Classification of Diseases (ICD)-9, ICD-10 [38], Medical Dictionary for Regulatory Activities (MedDRA) [39], and Systematised Nomenclature of Medicine (SNOMED) [40], but diagnosis or medications are associated with the payment of medical insurance, and use of classification schemas and terminology are at the discretion of clinicians at each site. Thus, the central coordinating centre will need

to monitor and standardise the use of EMRs and integrate data provided across sites. In addition, a vendor-neutral and platform-independent standard format, such as the CDISC Operational Data Model (ODM) [41] and the CDISC Study Data Tabulation Model (SDTM) [42], will be needed to archive, transfer, and integrate trial data. The advantage is that the EMR system would not need to be retained in the future to access the data or the audit trail [5].

Conclusion

We proposed a new clinical trial process model by integrating it with clinical pathways and EMRs, which is the primary use of EMRs in a clinical trial. In a single-centre trial selected for the pilot study, our new model was integrated with the routine documentation of clinical practice and the procedures of clinical trials. Therefore, redundant data entries for the trial were avoided, and the burden on the investigators posed by the trial was minimised.

The basis of our model is that the standardisation of clinical practice from clinical pathways can be applied as a treatment plan for a clinical trial; one primary use of the EMR system could be to provide data for clinical trials. The most prominent characteristic of our model is that many data management tasks that typically are performed by the central coordinating centre are moved to the participating sites. In effect, the EMRs replace the EDC system and the CDMS. To maintain efficient data quality control, it is important to execute data management near the site of the data occurrence. The earlier an error is detected in a clinical trial, the sooner and more easily and cheaply it can be rectified [3]. Conventionally, the period from when an investigator executes protocol treatment to when the trial data are transcribed in the CRFs and checked by the data manager of the central coordinating centre spans several days (e.g., mean 5 days; ranging 1–25 days in our centre). In contrast, when investigators added information to the EMRs in the test trial, the data were immediately available to the local data manager for checking, which allowed rapid resolution of any anomalies introduced. Such real-time availability of trial data should reduce the time and cost of conducting clinical trials.

In addition, in the eSDI proposal, the third scenario was called 'Single Source Concept' [5]: data need to be entered only once for multiple purposes (research, patient care, safety surveillance) within the context of existing regulations. The fourth scenario was called 'EMR Extraction and Investigator Verification': a clinician would check EMRs for the necessary data for the clinical trial and extract and transfer the data to a sponsor. We believe that our new model fits these scenarios and that we have demonstrated an implementation model for eClinical trials based on the eSDI proposal. According to the eSDI scenario, Title 21 Part 11 of the Code of Federal Regulations [43] starts at the point of the creation of a clinical research record. In other words, it is not necessary to apply these regulations to the medical records at the site. The clinical research record is created at the point of electronic signature signing. When data are extracted from EMRs as clinical trial data, the migration of the data from EMRs to the clinical trial database must be validated at the participating site. In addition, the sponsor has to produce documents on how the procedures of the clinical trial follow all appropriate regulations. Because of the direct extraction of the clinical trial data from EMRs, our model may eliminate or minimise the need for SDV. The audit plan should focus on the accuracy of the migration of data from EMRs to ensure that data are not changed in the extraction process and that patient confidentiality requirements are met [5]. We believe that by appropriating the efforts of SDV in favour of validating the clinical trial process, the costs can be reduced and the efficiency of clinical trials can be improved.

Acknowledgements

The authors would like to acknowledge the staff of the Department of Medical Informatics of Kyoto University Hospital and the Kyoto University EBM Research Centre for their generous support. Keiichi Yamamoto and Kenya Yamanaka contributed equally to this article.

Funding

This work was supported by Coordination, Support and Training Program for Translational Research of Ministry of Education, Culture, Sports, Science and Technology of Japan and Grants-in-Aid for Scientific Research of Japan (23790566).

References

1. **Embi PJ, Payne PR.** Clinical research informatics: Challenges, opportunities and definition for an emerging domain. *J Am Med Inform Assoc* 2009; **16**(3): 316–27.
2. **Zhengwu L, Jing S.** Clinical data management: Current status, challenges, and future directions from industry perspectives. *Open Access J Clin Trials* 2010; **2**: 93–105.
3. **Daniels Kush R.** *eClinical Trials: Planning and Implementation*. CenterWatch, Boston, MA, 2003, pp. 12, 38.
4. **McFadden E.** *Management of Data in Clinical Trials* (2nd edn). Wiley Interscience, Hoboken, NJ, 2007, pp. 33, 56, 80, 94.
5. **Clinical Data Interchange Standards Consortium (CDISC).** Leveraging the CDISC standards to facilitate the use of electronic source data within clinical trials (eSDI), 2006. Available at: http://www.cdisc.org/stuff/contentmgr/files/0/2f6eca8f0df7caac5bbd4fadfd76d575/miscdocs/esdi.pdf (accessed April 2011).

6. **Yamamoto K, Matsumoto S, Tada H,** *et al.* A data capture system for outcomes studies that integrates with electronic health records: Development and potential uses. *J Med Syst* 2008; **32**(5): 423–27.
7. **Kush R, Alschuler L, Ruggeri R,** *et al.* Implementing single source: The STARBRITE proof-of-concept study. *J Am Med Inform Assoc* 2007; **14**(5): 662–73.
8. **CDISC.** Healthcare link initiative, 2009. Available at: http://www.cdisc.org/healthcare-link (accessed April 2012).
9. **ASTER.** The ASTER Pilot Project: Improving the reporting of adverse events, 2009. Available at: http://www.asterstudy.com/index.php?option=com_content&;view=article&id=10:aster-description (accessed April 2012).
10. **Yamamoto K, Matsumoto S, Yanagihara K,** *et al.* A data-capture system for post-marketing surveillance of drugs that integrates with hospital electronic health records. *Open Access J Clin Trials* 2011; **3**: 21–26.
11. **Prokosch HU, Ganslandt T.** Perspectives for medical informatics. Reusing the electronic medical record for clinical research. *Methods Inf Med* 2009; **48**(1): 38–44.
12. **Wasserman RC.** Electronic medical records (EMRs), epidemiology, and epistemology: Reflections on EMRs and future pediatric clinical research. *Acad Pediatr* 2011; **11**(4): 280–87.
13. **Kristianson KJ, Ljunggren H, Gustafsson LL.** Data extraction from a semi-structured electronic medical record system for outpatients: A model to facilitate the access and use of data for quality control and research. *Health Inform J* 2009; **15**(4): 305–19.
14. **Lenz R, Blaser R, Beyer M,** *et al.* IT support for clinical pathways – Lessons learned. *Int J Med Inform* 2007; **76**(Suppl. 3): S397–402.
15. **Courtney L, Gordon M, Romer L.** A clinical path for adult diabetes. *Diabetes Educ* 1997; **23**(6): 664–71.
16. **US National Cancer Institute.** Common terminology criteria for adverse events (CTCAE) and common toxicity criteria (CTC), 2010. Available at: http://ctep.cancer.gov/protocolDevelopment/electronic_applications/ctc.htm (accessed April 2012).
17. **Matsumura Y, Kuwata S, Yamamoto Y,** *et al.* Template-based data entry for general description in medical records and data transfer to data warehouse for analysis. *Stud Health Technol Inform* 2007; **129**(Pt 1): 412–16.
18. **Henry SB, Douglas K, Galzagorry G, Lahey A, Holzemer WL.** A template-based approach to support utilization of clinical practice guidelines within an electronic health record. *J Am Med Inform Assoc* 1998; **5**(3): 237–44.
19. **Los RK, van Ginneken AM, van der Lei J.** OpenSDE: A strategy for expressive and flexible structured data entry. *Int J Med Inform* 2005; **74**(6): 481–90.
20. **Rose EA, Deshikachar AM, Schwartz KL, Severson RK.** Use of a template to improve documentation and coding. *Fam Med* 2001; **33**(7): 516–21.
21. **Chen R, Enberg G, Klein GO.** Julius: A template based supplementary electronic health record system. *BMC Med Inform Decis Mak* 2007; **7**: 10.
22. **Prat N.** A UML-based data warehouse design method. *Decis Support Syst* 2006; **42**(3): 1449–73.
23. **Grant A, Moshyk A, Diab H,** *et al.* Integrating feedback from a clinical data warehouse into practice organisation. *Int J Med Inform* 2006; **75**(3–4): 232–39.
24. **Rubin DL, Desser TS.** A data warehouse for integrating radiologic and pathologic data. *J Am Coll Radiol* 2008; **5**(3): 210–17.
25. **Wade TD, Hum RC, Murphy JR.** A Dimensional Bus model for integrating clinical and research data. *J Am Med Inform Assoc* 2011; **18**(Suppl. 1): i96–102.
26. **Gordon BD, Asplin BR.** Using online analytical processing to manage emergency department operations. *Acad Emerg Med* 2004; **11**(11): 1206–12.
27. **University Hospital Medical Information Network.** UMIN Clinical Trials Registry (UMIN-CTR), 2005. Available at: http://www.umin.ac.jp/ctr/ (accessed April 2012).
28. **Bruix J, Sala M, Llovet JM.** Chemoembolization for hepatocellular carcinoma. *Gastroenterology* 2004; **127**(5, Suppl. 1): S179–88.
29. **Yamanaka K, Hatano E, Narita M,** *et al.* Comparative study of cisplatin and epirubicin in transcatheter arterial chemoembolization for hepatocellular carcinoma. *Hepatol Res* 2011; **41**: 303–09.
30. **Forner A, Ayuso C, Varela M,** *et al.* Evaluation of tumor response after locoregional therapies in hepatocellular carcinoma: Are response evaluation criteria in solid tumors reliable?. *Cancer* 2009; **115**: 616–23.
31. **Kudo M, Kubo S, Takayasu K,** *et al.* Response Evaluation Criteria in Cancer of the Liver (RECICL) proposed by the Liver Cancer Study Group of Japan (2009 Revised Version). *Hepatol Res* 2010; **40**(7): 686–92.
32. **Brown JM, Haining SA, Hale JM.** Views on local data management in cancer clinical trials. *Clin Oncol (R Coll Radiol)* 1997; **9**(6): 403–06.
33. **Tunis SR, Stryer DB, Clancy CM.** Practical clinical trials: Increasing the value of clinical research for decision making in clinical and health policy. *JAMA* 2003; **290**(12): 1624–32.
34. **Joo JH, Morales KH, de Vries HF, Gallo JJ.** Disparity in use of psychotherapy offered in primary care between older African-American and white adults: Results from a practice-based depression intervention trial. *J Am Geriatr Soc* 2010; **58**(1): 154–60.
35. **Tunis SR, Benner J, McClellan M.** Comparative effectiveness research: Policy context, methods development and research infrastructure. *Stat Med* 2010; **29**(19): 1963–76.
36. **Rostami R, Nahm M, Pieper CF.** What can we learn from a decade of database audits? The Duke Clinical Research Institute experience, 1997–2006. *Clin Trials* 2009; **6**(2): 141–50.
37. **Pan JJ, Nahm M, Wakim P,** *et al.* A centralized informatics infrastructure for the National Institute on Drug Abuse Clinical Trials Network. *Clin Trials* 2009; **6**(1): 67–75.
38. **WHO.** International Classification of Diseases (ICD), 2007. Available at: http://www.who.int/classifications/icd/en/ (accessed April 2012).
39. **MedDRA MSSO.** MedDRA MSSO, 2011. Available at: http://www.meddramsso.com/ (accessed April 2012).
40. **U.S. National Library of Medicine.** SNOMED Clinical Terms, 2009. Available at: http://www.nlm.nih.gov/research/umls/Snomed/snomed_main.html (accessed April 2012).
41. **Clinical Data Interchange Standards Consortium (CDISC).** Operational Data Model, 2011. Available at: http://www.cdisc.org/odm (accessed April 2012).
42. **Clinical Data Interchange Standards Consortium (CDISC).** Study Data Tabulation Model, 2011. Available at: http://www.cdisc.org/sdtm (accessed April 2012).
43. **U.S. Food and Drug Administration.** CFR: Code of Federal Regulations Title 21, 2011. Available at: http://www.accessdata.fda.gov/scripts/cdrh/cfdocs/cfcfr/cfrsearch.cfm?cfrpart=11 (accessed April 2012).

Am J Transl Res 2012;4(1):52-59
www.ajtr.org /ISSN:1943-8141/AJTR1110002

Original Article

An exploratory clinical trial for combination wound therapy with a novel medical matrix and fibroblast growth factor in patients with chronic skin ulcers: a study protocol

Naoki Morimoto[1], Kenichi Yoshimura[2], Miyuki Niimi[2], Tatsuya Ito[3], Harue Tada[2], Satoshi Teramukai[2], Toshinori Murayama[4], Chikako Toyooka[4], Satoru Takemoto[1], Katsuya Kawai[1], Masayuki Yokode[4], Akira Shimizu[3], Shigehiko Suzuki[1]

[1]Department of Plastic and Reconstructive surgery, Graduate School of Medicine, Kyoto University; [2]Department of Clinical Trial Design and Management, Translational Research Center, Kyoto University Hospital; [3]Department of Experimental Therapeutics, Translational Research Center, Kyoto University Hospital; [4]Department of Clinical Innovative Medicine, Translational Research Center, Kyoto University Hospital, Japan.

Received October 17, 2011; accepted November 20, 2011; Epub January 5, 2012; Published January 15, 2012

Abstract: Background: Chronic skin ulcers such as diabetic ulcers and venous leg ulcers are increasing and are a costly problem in health care. We have developed a novel artificial dermis, collagen/gelatin sponge (CGS), that is capable of the sustained release of basic fibroblast growth factor (bFGF) for more than 10 days. The objective of this study was to investigate the safety and efficacy of CGS impregnated with bFGF in the treatment of chronic skin ulcers. Methods/Design: Seventeen patients (≥ 20 years of age) with chronic skin ulcers that have not healed by conventional therapy for at least 4 weeks are being recruited. Patients will be applied with CGS impregnated with bFGF of 7 μg/cm^2 or 14 μg/cm^2 after debridement, and the wound bed improvement will be assessed 14 days after application. "Wound bed improvement" is defined as a granulated and epithelialized area on Day 14 in proportion to the baseline wound area after debridement of 50% or higher. Patients will be followed up until 28 days after application to observe the adverse events related to the application of CGS. Conclusion: This study has been designed to address the safety and efficacy of CGS impregnated with bFGF. If successful, this intervention may be an alternative to bioengineered skin substitutes and lead to substantial and important changes in the management of chronic skin ulcers such as diabetic ulcers and venous ulcers.

Keywords: Artificial dermis, basic fibroblast growth factor, skin ulcers, sustained release

Introduction

Non-healing or chronic skin ulcers are an increasing and costly problem in health care [1-4]. Chronic skin ulcers are caused by diabetes mellitus, venous insufficiency, pressure sores, collagen disease, trauma, or radiation. With the development of tissue engineering and advances in cell and molecular biology, novel bioengineered skin substitutes and genetically derived growth factors offer promise in the treatment of chronic skin ulcers [5-7]; however, there are still issues that remain to be solved in the treatment of those ulcers. Diabetic foot ulcers and venous leg ulcers are frequent and costly complications of their underlying diseases. The prevalence of foot ulcers ranges from 4% to 10% among persons diagnosed with diabetes mellitus [3, 4] and the annual population-based incidence of 1.0% to 5% [1, 3, 4], and the lifetime incidence may be as high as 25% [3, 4]. More than 15% of all ulcers result in some form of amputation [3, 4]. According to a previous report, venous leg ulcers recurred in 72% of cases and skin ulcers from other causes recurred in 45% of cases [2], and another report described recurrence in 48% of cases one year after skin grafting [8].

We developed a bilayered acellular artificial dermis composed of an upper silicone sheet and a lower collagen sponge [9, 10] by modifying the material described by Yannas and Burke [11, 12]. Artificial dermis has been used in the treatment of full-thickness skin defects resulting

from burns, trauma injuries and tumor removal. After application of the artificial dermis to skin defects, fibroblasts and capillaries penetrate and proliferate in the collagen sponge and dermis-like tissue is formed after degradation of the collagen sponge [9-11]. However, it is difficult to apply ordinary artificial dermis to chronic skin ulcers, because the artificial dermis has no resistance to infection and is easily infected before the infiltration of capillaries into the inner collagen sponge.

Basic fibroblast growth factor (bFGF), which was identified in 1974, promotes the proliferation of fibroblasts and capillary formation and accelerates tissue regeneration [13, 14]. In Japan, human recombinant bFGF (FIBRAST SPRAY; Kaken Pharmaceutical, Tokyo, Japan) has been used clinically for chronic skin ulcers since 2001, and its clinical effectiveness has been demonstrated [7, 15]. Recently, combination therapy involving bFGF and artificial dermis has been reported to accelerate dermis-like tissue formation in the treatment of traumatic wounds [16]. In addition, this combination therapy was reported to be effective for chronic skin ulcers such as diabetic foot ulcers, ulcers caused by collagen disease, oral steroids and arteriosclerosis obliterans [17-19]. This is because bFGF causes the proliferation of fibroblasts and strongly promotes angiogenesis in artificial dermis, leading to the early formation of dermis-like tissue and promoting wound healing; however, this combination therapy has not become the standard treatment of chronic ulcers, because once daily topical administration of bFGF is required to achieve the expected effect because the artificial dermis has no ability to retain bFGF and it rapidly diffuses away from the applied site and is also inactivated quickly after its administration in vivo; thus, significant burdens are imposed on both medical staff and patients for daily application. For these reasons, we have developed a novel artificial dermis, collagen/gelatin sponge (CGS), containing a 10wt% concentration of acidic gelatin that is capable of the sustained release of positively charged growth factors such as bFGF for more than 10 days in vivo [20]. In our previous study, CGS was used as a scaffold for dermal regeneration, the same as conventional artificial dermis, and degraded after application to the wound site, being replaced by dermis-like tissue [20].

In our previous studies to apply CGSs impregnated with 7 μg/cm^2 or 14 μg/cm^2 of bFGF to full-thickness skin defects of normal mice and decubitus created on diabetic mice, the time required for regeneration of dermis-like tissue in mice treated with CGSs with bFGF was half to one third of the time required in mice treated with conventional artificial dermis alone [21]. In another study using mucosal defects of dog palates, CGSs impregnated with 7 μg/cm^2 bFGF accelerated the regeneration of palatal mucosa with good neovascularization and showed less contracture [22]. Alternative therapies for chronic skin ulcers have been proposed, such as tissue engineering products, growth factors, and hyperbaric oxygen therapy [23, 24]. Hyperbaric oxygen therapy is a systemic therapy; therefore, it can be combined with CGSs. The mechanism of action of tissue engineering products is considered mainly as the effects of cytokines and growth factors secreted by living cells [25]. Our CGS impregnated with bFGF can sustain and release bFGF in a controlled manner; therefore, the effectiveness of CGS will either equal or surpass and be competitive in cost to tissue engineering products. Moreover, both CGS and bFGF can be stored at room temperature and used whenever needed. Usually, growth factors must be applied once or twice a day because of their rapid inactivation after administration, and CGS with bFGF will be superior in this respect.

In view of the above, combination therapy with this novel collagen-based artificial dermis (CGS) and bFGF is anticipated to be comparably minimally invasive and effective to tissue engineering products to promote wound healing even in patients with chronic skin ulcers. Thus, we propose to investigate the safety and efficacy of this combination therapy in the treatment of chronic skin ulcers.

Materials and methods

Primary objective

The objective of this study is to evaluate the safety and efficacy of CGS impregnated with bFGF in the treatment of chronic skin ulcers that are not expected to heal with conventional treatments.

Methods and design

Open-label, randomized, multiple dose, con-

trolled clinical trial.

Design

Two groups, a low-dose and high-dose bFGF group, have been set (**Figure 1**). In the initial step (Step 1), three patients will be enrolled in the low-dose group. After confirming the safety in the low-dose group, patients will be randomized to the low-dose or high-dose bFGF group in Step 2. Randomization-based comparison between dose groups can achieve significant improvements in accuracy and lack of bias. This comparison can provide useful information for designing and conducting future trials.

Setting and participants

This study is being conducted at Kyoto University Hospital. Patients with chronic skin ulcers are referred by physicians and also identified through a number of wound care clinics in Kyoto Prefecture and surrounding prefectures.

Inclusion criteria

1). Patients aged 20 years or older at informed consent. 2). Presence of chronic skin ulcers as below: not healing for at least 4 weeks with conventional treatments; skin graft is not expected to take; can be completely covered by a 70 mm × 100 mm device. 3). If chronic skin ulcers are present on lower extremities, the skin perfusion pressure must be ³ 30 mmHg at a site proximal or distal to those ulcers. 4). Written informed consent.

Exclusion criteria

1). Have any of the following systemic diseases: uncontrolled diabetes mellitus (defined by HbA1c ³ 10%) according to latest laboratory data obtained within 28 days before registration); requiring continued use of oral corticosteroid therapy (> 20 mg/day prednisolone equivalent); a history of malignant tumor with disease-free interval of 5 years or less. 2). Have a history of allergy to porcine-derived products, collagen, gelatin, bFGF, anesthetic drugs, disinfectants, etc. 3). Have participated in another clinical trial/study within the past three months. 4). Have participated in this study previously. 5). Women meeting any of the following: do not agree to avoid pregnancy during the study; currently pregnant or possibly pregnant; currently breastfeeding. 6). Other patients judged by the investigator or sub-investigator to be inappropriate as a subject of this study.

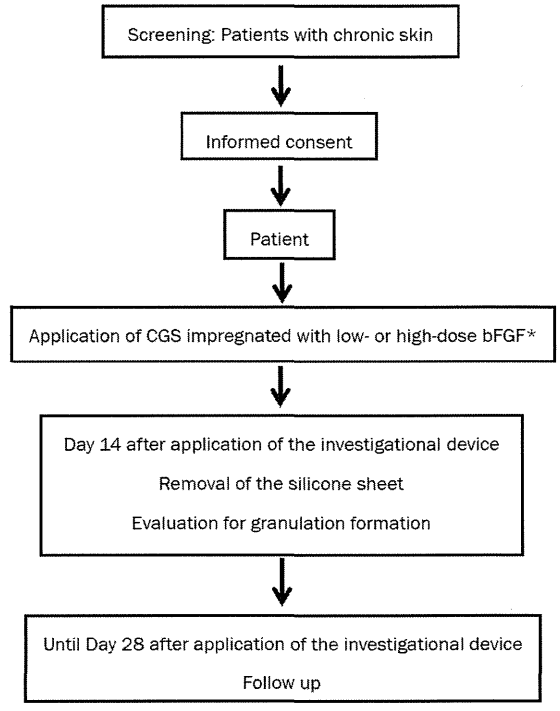

*: Step 1 (non-randomized): low-dose bFGF (n=3): Step 2 (randomized): low-dose bFGF (n=7) and high-dose bFGF (n=7)

Randomization

In Step 2, patients will be randomized to either the low-dose or high-dose bFGF group at a ratio of 1:1 without stratification. Randomization will be performed using a computer-generated random sequence to ensure equal allocation to the two dose groups by a statistician of the independent data center (Department of Clinical Trial Design and Management, Translational Research Center, Kyoto University Hospital).

Interventions

Preparations of CGS impregnated with bFGF

CGS is the modification of conventional bilayered artificial dermis (Pelnac; Gunze Co., Ltd, Kyoto, Japan) and consists of an upper silicone sheet (0.1mm in thickness) and lower sponge (3 mm in thickness) [20]. In this study, the lar-

ger CGS (82 mm × 120 mm) will be used. Two different dose bFGF concentrations of 7 μg/cm^2 (low dose) or 14 μg/cm^2 (high dose) will be used. On the day of study therapy, the investigator or sub-investigator will prepare CGS impregnated with bFGF in the operating room

Application of CGS impregnated with bFGF

This therapy will be started within 28 days of enrollment. After debridement of the chronic skin ulcers, CGS impregnated with bFGF of 7 μg/cm^2 or 14 μg/cm^2 and cut according to the shape of the wound will be applied and sutured to surrounding skin.

Dressing changes and silicone sheet removal

After the application of CGS, dressings will be changed as necessary. Patients will be hospitalized until Day 7 to ensure stabilization of the applied CGS and may be discharged on Day 8 after application according to the condition of the wound. On Day 14 after application, the sutures and silicone sheet of CGS will be removed. After silicone film removal, subsequent therapy may be started.

Subsequent therapy

The use of bFGF or another collagen-based artificial skin will be prohibited until Day 28 after application. The use of ointments, wound dressings and skin grafting will be allowed. After completion of the study period (Day 29 after investigational device application and onward), no particular restrictions will be imposed.

Digital photograph for healing assessment

Using a digital camera, digital images of the wounds will be taken with a calibrator (CASMATCH; BEAR Medic Corp., Tokyo, Japan) placed on the skin adjacent to the wound. The color and size of image will be adjusted using the CASMATCH and image editing software (Adobe Photoshop; Adobe Systems) to assess the wound and granulation areas. As with the primary endpoint, the granulation tissue evaluation committee members will assess the wound and granulation areas.

Primary endpoint

The primary endpoint is "wound bed improvement."

Granulation tissue is wound connective tissue, which forms at the beginning of wound healing [26]. This highly fibrous tissue is usually pink because numerous small capillaries invade granulation tissue to supply oxygen and nutrients. The appearance of granulation tissue is a good sign of healing because when a wound starts granulating, it means that the healing process of the wound is starting [26-28]. The area of granulation tissue will be measured as the granulation formation area in this study. An unhealed area is defined as an area with no epithelialization and no granulation formation. In this study, the percentage of wound bed improvement is defined as the value (%) calculated from the sum of the granulated and epithelialized areas on Day 14 divided by the baseline wound area after debridement on Day 0 multiplied by 100, and the patient is diagnosed with wound bed improvement if the wound bed improvement indicator is 50% or higher. The use of 50% or more as the cutoff for the wound bed improvement indicator is based on the pressure ulcer healing assessment scale by the Japanese Society of Pressure Ulcers [28, 30, 31].

Secondary endpoints

1). Adverse events and adverse reactions. 2). Percentage of "wound bed improvement". 3). Percentage of wound reduction: The percentage of wound area reduction is defined as the value (%) calculated from the wound area of the ulcer on Day 14 divided by the baseline wound area after debridement on Day 0 multiplied by 100. 4). Percentage of granulation area: The percentage of granulation area is defined as the value (%) calculated from the granulation area divided by the wound area on Day 14 multiplied by 100.

Blinding

The baseline wound area, the wound area on Day 14 and the granulation area on Day 14 will be independently measured under blinding by central review. Patients will be unblinded, and unblinded investigators will apply CGSs and change dressings.

Sample size

This study will be conducted to determine whether CGS impregnated with bFGF is promising for the treatment of chronic skin ulcers, as evaluated based on wound bed improvement as

Table 1. Schedule of study assessments and evaluations

	Treatment			Observation
Clinical assessments, testing and investigations	Day of enrollment	Day of application/ reapplication	← → Day of silicone sheet removal (Day 14)	Day 28 after application/ reapplication
Clinical history	○			
Physical examination	○			
Eligibility criteria check	○			
Informed consent	○			
Blood test	○		○	○
Skin perfusion pressure	○			
Investigational device application		○		
Clinical assessment of the wound	○	○	○	○
Digital photograph of wound	○	○	○	○
Wound evaluation			●	
Data submission of treatment and AE etc.		○	○	○
Observation of AE		○	← ○ → ○	○

○: required; ●: Wound area measurements, granulation area measurements (wound for efficacy evaluation and wounds for study therapy)

the primary endpoint. Primary analyses will be conducted using all data treated with CGS in Step 1 and Step 2. Since debridement and conventional therapies rarely lead to wound bed improvement in this patient population, the null hypothesis tested in this study is that the proportion of patients with wound bed improvement is 10% or less. The null hypothesis is also supported by previous trials [32-34]. In consideration of the minimum clinically important difference, the expected proportion of patients with wound bed improvement in this study is set to 50% or more. When exact testing based on binomial distribution is conducted with a one-sided significance level of 2.5% and a statistical power of 90% or higher, the required number of subjects is 14. Allowing for a drop-out rate of 20% or less, the total number of patients for registration is 17, specifically 3 patients in Step 1 and 14 patients in Step 2.

Study schedule

The schedule of study assessments and evaluations is shown in **Table 1**. The study period will be from the day of informed consent to 28 days after investigational device application. The study period will be from the day of investigational device application to 28 days after investigational device application. Data to evaluate the efficacy and safety of this study will be collected at enrollment, baseline, and Day 14 of the treatment phase and Day 28 of the observation phase.

Statistical analysis

Patients who have been registered for the study and who have undergone investigational device application at least once will be included in the full analysis set (FAS) and the safety analysis

set. From the FAS, however, patients will be excluded if they have serious protocol violations or International Conference on Harmonization Guidelines for Good Clinical Practice (ICH-GCP) violations (failure to obtain consent, major study procedure violations) or if they are found to be ineligible after registration.

Wound bed improvement

Wound bed improvement is the primary endpoint of this study. The primary analysis will be conducted for the FAS using exact test based on binomial distribution with a null proportion of 10% and a one-sided significance level of 2.5%. The 95% confidence interval of the proportion of patients with wound bed improvement will be calculated using an exact method based on binomial distribution.

Percentage of wound bed improvement, would reduction and granulation area

Using the FAS, the descriptive statistics will be calculated. The interval estimation will be conducted under the assumption that this endpoint follows normal distribution.

Adverse events related to the application of the device

Using the safety analysis set, the frequency/incidence of adverse events and adverse events that can be causally related to the investigational device in the safety analysis set will be calculated by event and severity.

Ethical considerations

This study is being conducted in compliance with the ICH-GCP and in agreement with the latest revision of the Declaration of Helsinki, Pharmaceutical Affairs Law and all applicable Japanese laws and regulations, as well as any local laws and regulations and all applicable guidelines. This protocol and any amendments have Institutional Review Board approval at Kyoto University Hospital.

Subject consent

Informed consent will be obtained from all potential study participants using the IRB-approved informed consent form. The clinical investigator informs the potential study subject of all pertinent aspects of the study. The subject must sufficiently understand the contents of the information form before providing written consent. The consent form must be dated and signed by both the investigator and the participant. Subjects are also informed that their medical care will not be affected if they do not choose to participate in this study. The consent form will be retained at Kyoto University Hospital and the information form and a copy of the consent form will be handed to the participant. Whenever the investigator obtains information that may affect the participant's willingness to continue participation in the study, the investigator or sub-investigator will immediately inform the participant and record this, and reconfirm the participant's willingness to continue participation in the study.

Adverse events

This study is being conducted according to the ICH-GCP. Adverse events and serious adverse events information will be documented according to the Medical Dictionary for Regulatory Activities (MedDRA) version 14.0.

Results and discussion

This study has been designed to address the safety and efficacy of novel treatment for chronic skin ulcers using a modified artificial dermis, CGS, that can sustain bFGF. This study will be the first randomized controlled trial to evaluate the efficacy of CGS and the appropriate concentration of bFGF impregnation for treatment of increasing non-healing ulcers. Some bioengineered skin substitutes that provide growth factors secreted by living cells have been reported to be effective for chronic skin ulcers, although they are costly and access is limited to only a few areas and countries. Both CGS and bFGF are freeze-dried and can be kept well and stored at room temperature. These are off-the-shelf products and the procedure of impregnation is simple; therefore, we can use this combination therapy anywhere when needed. If successful, this intervention may lead to substantial and important changes in the management of chronic skin ulcers, such as diabetes ulcers and venous leg ulcers

Acknowledgements

This work was supported by a grant from the

Japan Science and Technology Agency.

Address correspondence to: Dr. Naoki Morimoto, Department of Plastic and Reconstructive Surgery, Graduate School of Medicine, Kyoto University, 54, Kawahara-cho Shogoin, Sakyo-ku, Kyoto 606-8507, Japan Tel: +81-75-751-3613; Fax: + 81-75-751-4340; E-mail: mnaoki22@kuhp.kyoto-u.ac.jp

References

[1] Vuorisalo S, Venermo M, Lepäntalo M. Treatment of diabetic foot ulcers. J Cardiovasc Surg (Torino) 2009; 50: 275-291.

[2] Bergqvist D, Lindholm C, Nelzen O. Chronic leg ulcers: the impact of venous disease. J Vasc Surg 1999; 29: 752-755.

[3] Singh N, Armstrong DG, Lipsky BA. Preventing foot ulcers in patients with diabetes. JAMA 2005; 293: 217-228.

[4] Wu SC, Driver VR, Wrobel JS, Armstrong DG. Foot ulcers in the diabetic patient, prevention and treatment. Vasc Health Risk Manag 2007; 3: 65-76.

[5] Ehrenreich M, Ruszczak Z. Update on tissue-engineered biological dressings. Tissue Eng 2006; 12: 2407-2424.

[6] Mason C, Manzotti E. Regenerative medicine cell therapies: numbers of units manufactured and patients treated between 1988 and 2010. Regen Med 2010; 5: 307-313.

[7] Uchi H, Igarashi A, Urabe K, Koga T, Nakayama J, Kawamori R, Tamaki K, Hirakata H, Ohmura T, Furue M. Clinical efficacy of basic fibroblast growth factor (bFGF) for diabetic ulcer. Eur J Dermatol 2009; 19: 461-468.

[8] Trier WC, Peacock EE Jr, Madden JW. Studies on the effectiveness of surgical management of chronic leg ulcers. Plast Reconstr Surg 1970; 45: 20-23.

[9] Suzuki S, Matsuda K, Issiki N, Tamada Y, Ikada Y. Experimental study of a newly developed bilayer artificial skin. Biomaterials 1990; 11: 356-360.

[10] Suzuki S, Matsuda K, Isshiki N, Tamada Y, Yoshioka K, Ikada Y. Clinical evaluation of a new bilayer 'artificial skin' composed of collagen sponge and silicone layer. Br J Plast Surg 1990; 43: 47-54.

[11] Yannas IV, Orgill DP, Burke JF. Template for skin regeneration. Plast Reconstr Surg 2011; 127: 60S-70S.

[12] Yannas IV, Burke JF. Design of an artificial skin. I. Basic design principles. J Biomed Mater Res 1980; 14: 65-81.

[13] Gospodarowicz D. Localization of a fibroblast growth factor and its effect alone and with hydrocortisone on 3T3 cell growth. Nature 1974; 249: 123-127.

[14] Hom DB, Unger GM, Pernell KJ, Manivel JC. Improving surgical wound healing with basic fibroblast growth factor after radiation. Laryngoscope 2005; 115: 412-422.

[15] Akita S, Akino K, Imaizumi T, Hirano A. Basic fibroblast growth factor accelerates and improves second-degree burn wound healing. Wound Repair Regen 2008; 16: 635-641.

[16] Muneuchi G, Suzuki S, Moriue T, Igawa HH. Combined treatment using artificial dermis and basic fibroblast growth factor (bFGF) for intractable fingertip ulcers caused by atypical burn injuries. Burns 2005; 31: 514-517.

[17] Akita S, Akino K, Tanaka K, Anraku K, Hirano A. A basic fibroblast growth factor improves lower extremity wound healing with a porcine-derived skin substitute. J Trauma 2008; 64: 809-815.

[18] Ito K, Ito S, Sekine M, Abe M. Reconstruction of the soft tissue of a deep diabetic foot wound with artificial dermis and recombinant basic fibroblast growth factor. Plast Reconstr Surg 2005; 115: 567-572

[19] Fujioka M. Combination treatment with basic fibroblast growth factor and artificial dermis improves complex wounds in patients with a history of long-term systemic corticosteroid use. Dermatol Surg 2009; 35: 1422-1425.

[20] Takemoto S, Morimoto N, Kimura Y, Taira T, Kitagawa T, Tomihata K, Tabata Y, Suzuki S. Preparation of collagen/gelatin sponge scaffold for sustained release of bFGF. Tissue Eng Part A 2008; 14: 1629-1638.

[21] Kanda N, Morimoto N, Takemoto S, Ayvazyan AA, Kawai K, Sakamoto Y, Taira T, Suzuki S. Efficacy of Novel Collagen/Gelatin Scaffold With Sustained Release of Basic Fibroblast Growth Factor for Dermis-like Tissue Regeneration. Ann Plast Surg 2011. [Epub ahead of print]

[22] Ayvazyan AA, Morimoto N, Kanda N, Kawai K, Sakamoto Y, Taira T, Suzuki S. Collagen-gelatin scaffold impregnated with bFGF accelerates palatal wound healing of palatal mucosa in dogs. J Surgical Res 2011; 171: 247-257.

[23] Langer A, Rogowski W. Systematic review of economic evaluations of human cell-derived wound care products for the treatment of venous leg and diabetic foot ulcers. BMC Health Serv Res 2009; 9: 115.

[24] O'Reilly D, Linden R, Fedorko L, Tarride JE, Jones WG, Bowen JM, Goeree R. A prospective, double-blind, randomized, controlled clinical trial comparing standard wound care with adjunctive hyperbaric oxygen therapy (HBOT) to standard wound care only for the treatment of chronic, non-healing ulcers of the lower limb in patients with diabetes mellitus: a study protocol. Trials 2011; 12: 69.

[25] Wong T, McGrath JA, Navsaria H. The role of fibroblasts in tissue engineering and regeneration. Br J Dermatol 2007; 156: 1149-1155.

[26] Shaw TJ, Martin P. Wound repair at a glance. J Cell Sci 2009; 122: 3209-3213.

[27] Martin P. Wound Healing-Aiming for Perfect

Skin Regeneration. Science 1997; 276: 75-81.
[28] Sanada H, Moriguchi T, Miyachi Y, Ohura T, Nakajo T, Tokunaga K, Fukui M, Sugama J, Kitagawa A. Reliability and validity of DESIGN, a tool that classifies pressure ulcer severity and monitors healing. J Wound Care 2004; 13: 13-18.
[29] Lavery LA, Barnes SA, Keith MS, Seaman JW Jr, Armstrong DG. Prediction of healing for postoperative diabetic foot wounds based on early wound area progression. Diabetes Care 2008; 31: 26-29.
[30] Japanese Society of Pressure Ulcers. Guideline for Local Treatment of Pressure Ulcers 2005.
[31] Japanese Society of Pressure Ulcers. Guideline for Prevention and Management of Pressure Ulcers. 2009.
[32] Veves A, Falanga V, Armstrong DG, Sabolinski ML. Graftskin, a human skin equivalent, is effective in the management of noninfected neuropathic diabetic foot ulcers: a prospective randomized multicenter clinical trial. Diabetes Care 2001; 24: 290-295.
[33] Cardinal M, Eisenbud DE, Armstrong DG, Zelen C, Driver V, Attinger C, Phillips T, Harding K. Serial surgical debridement: a retrospective study on clinical outcomes in chronic lower extremity wounds. Wound Repair Regen 2009; 17: 306-311.
[34] Armstrong DG, Lavery LA. Negative pressure wound therapy after partial diabetic foot amputation: a multicentre, randomised controlled trial. Lancet 2005; 366: 1704-1710.

ORIGINAL RESEARCH

American Heart Association | American Stroke Association.

MicroRNA-33 Deficiency Reduces the Progression of Atherosclerotic Plaque in ApoE$^{-/-}$ Mice

Takahiro Horie, MD, PhD; Osamu Baba, MD; Yasuhide Kuwabara, MD, PhD; Yoshimasa Chujo, MD; Shin Watanabe, MD, PhD; Minako Kinoshita, MD, PhD; Masahito Horiguchi, MD, PhD; Tomoyuki Nakamura, MD, PhD; Kazuhisa Chonabayashi, MD, PhD; Masakatsu Hishizawa, MD, PhD; Koji Hasegawa, MD, PhD; Noriaki Kume, MD, PhD; Masayuki Yokode, MD, PhD; Toru Kita, MD, PhD; Takeshi Kimura, MD, PhD; Koh Ono, MD, PhD

Background—Cholesterol efflux from cells to apolipoprotein A-I (apoA-I) acceptors via the ATP-binding cassette transporters ABCA1 and ABCG1 is thought to be central in the antiatherogenic mechanism. MicroRNA (miR)-33 is known to target ABCA1 and ABCG1 in vivo.

Methods and Results—We assessed the impact of the genetic loss of miR-33 in a mouse model of atherosclerosis. MiR-33 and apoE double-knockout mice (miR-33$^{-/-}$*Apoe*$^{-/-}$) showed an increase in circulating HDL-C levels with enhanced cholesterol efflux capacity compared with miR-33$^{+/+}$*Apoe*$^{-/-}$ mice. Peritoneal macrophages from miR-33$^{-/-}$*Apoe*$^{-/-}$ mice showed enhanced cholesterol efflux to apoA-I and HDL-C compared with miR-33$^{+/+}$*Apoe*$^{-/-}$ macrophages. Consistent with these results, miR-33$^{-/-}$*Apoe*$^{-/-}$ mice showed reductions in plaque size and lipid content. To elucidate the roles of miR-33 in blood cells, bone marrow transplantation was performed in these mice. Mice transplanted with miR-33$^{-/-}$*Apoe*$^{-/-}$ bone marrow showed a significant reduction in lipid content in atherosclerotic plaque compared with mice transplanted with miR-33$^{+/+}$*Apoe*$^{-/-}$ bone marrow, without an elevation of HDL-C. Some of the validated targets of miR-33 such as RIP140 (NRIP1) and CROT were upregulated in miR-33$^{-/-}$*Apoe*$^{-/-}$ mice compared with miR-33$^{+/+}$*Apoe*$^{-/-}$ mice, whereas CPT1a and AMPKα were not.

Conclusions—These data demonstrate that miR-33 deficiency serves to raise HDL-C, increase cholesterol efflux from macrophages via ABCA1 and ABCG1, and prevent the progression of atherosclerosis. Many genes are altered in miR-33-deficient mice, and detailed experiments are required to establish miR-33 targeting therapy in humans. (***J Am Heart Assoc.*** **2012;1: e003376 doi: 10.1161/JAHA.112.003376)**

Key Words: ABCA1 • ABCG1 • atherosclerosis • HDL-C • microRNA

Although the lowering of LDL cholesterol (LDL-C) with the use of statins has revolutionized the treatment of atherosclerotic cardiovascular disease, statins can only reduce the risk of cardiovascular events by up to 50% depending on the disease status and the amount of statin used, which still leaves a large burden of residual disease risk.[1–3] Recent studies have shown that HDL cholesterol (HDL-C) levels under statin treatment remain an independent predictor of the risk of cardiovascular events in patients who have been treated with statins to lower LDL-C levels[4] and that HDL-C levels at baseline are a strong predictor of 12-month morbidity and mortality from cardiovascular events in patients on statins with low LDL-C levels undergoing stent placement for acute coronary syndromes.[5] Thus, clinical and epidemiological studies have consistently shown that there is an inverse relationship between HDL-C concentration and cardiovascular risk. In fact, a 1 mg/dL (0.026 mmol/L) increment in HDL-C levels was associated with a significant decrease in the risk of coronary heart disease of 2% in men and 3% in women.[6] All these data led us to the idea that the development of therapies that raise HDL-C is necessary to reduce cardiovascular diseases in the midst of the "statin era" in the management of atherosclerosis. Transgenic mice that

From the Departments of Cardiovascular Medicine (T.H., O.B., Y.K., Y.C., S.W., M.K., M. Horiguchi, N.K., T. Kimura, K.O.), Hematology and Oncology (K.C., M. Hishizawa), and Clinical Innovative Medicine, Translational Research Center (T.H., M.Y.), Graduate School of Medicine, Kyoto University, Kyoto, Japan; Department of Pharmacology, Kansai Medical University, Moriguchi, Osaka, Japan (T.N.); Division of Translational Research, Clinical Research Institute, Kyoto Medical Center, Kyoto, Japan (K.H.); Department of Cardiovascular Medicine, Kobe City Medical Center General Hospital, Kobe, Japan (T. Kita).

Drs Horie and Baba contributed equally to this article.

Correspondence to: Koh Ono, MD, PhD, Department of Cardiovascular Medicine, Graduate School of Medicine, Kyoto University, Kyoto, 54 Shogoinkawahara-cho, Sakyo-ku, Kyoto, 606-8507, Japan. E-mail: kohono@kuhp.kyoto-u.ac.jp

Received August 14, 2012; accepted September 28, 2012.

overexpress apoA-I and the infusion of apoA-I/phospholipid complexes in humans are associated with reduced progression or regression of atherosclerosis.[7–9] These observations have suggested that HDL-C-raising therapies might be an effective way to reduce the residual risk of cardiovascular diseases in patients who are being treated with current therapies.

The identification of ATP-binding cassette transporter A1 (ABCA1) as a rate-limiting factor in HDL-C biogenesis suggested that increased ABCA1 activity could inhibit atherosclerosis. Studies in mice in which the *Abca1* locus is either deleted or overexpressed generally have supported the hypothesis that ABCA1 significantly prevents atherosclerosis by maintaining circulating HDL-C levels and cellular cholesterol efflux.[10–13] Tissue-specific knockouts of the *Abca1* locus were generated and revealed that liver and macrophage ABCA1 both play roles in preventing atherosclerosis.[14] ABCA1 modulates cell-surface cholesterol levels, inhibits its partitioning into lipid rafts, and decreases the responsiveness of inflammatory signals from innate immune receptors. Moreover, ABCA1 has been reported to act directly as an anti-inflammatory receptor independent of its lipid transport activities.[15] Therefore, augmentation of the function of ABCA1 might be a beneficial therapeutic approach.

MicroRNA (miR) is small, nonprotein-coding RNA that binds to specific mRNA and inhibits translation or promotes mRNA degradation. Recent reports, including ours, have indicated that miR-33 controls cholesterol homeostasis based on knockdown experiments using antisense technology.[16–18] Moreover, antisense inhibition of miR-33 resulted in a regression of the atherosclerotic plaque volume in LDL-receptor-deficient mice.[19] Antisense inhibition of miRNA function is an important tool for elucidating miRNA biology and evaluating its therapeutic potential. However, to determine the organ-/cell-type-specific function of miRNA over the long term in vivo, studies on miRNA-deficient mice and the analysis of specific organ/cell types from these mice are needed, especially for the development of therapeutic strategies for chronic diseases, such as atherosclerosis, dyslipidemia, and metabolic syndrome.

In the present study, we crossed miR-33-deficient mice (miR-33$^{-/-}$) with apoE-deficient mice (*Apoe*$^{-/-}$) to examine the impact of miR-33 deletion on the progression of atherosclerosis and demonstrated that genetic loss of miR-33 raises circulating HDL-C and decreases atherosclerotic plaque size. Furthermore, loss of leukocyte miR-33 significantly reduced the lipid content in atherosclerotic plaque. Our results indicate that miR-33 deficiency raises both HDL-C and macrophage cholesterol efflux and strongly suggest that miR-33 should be considered as a potential target for the prevention of atherosclerosis. However, some of the previously validated targets of miR-33, such as RIP140 and CROT, were upregulated in miR-33$^{-/-}$*Apoe*$^{-/-}$ mice compared with miR-33$^{+/+}$*Apoe*$^{-/-}$ mice, whereas CPT1a and AMPKα were not. Moreover, the effect of miR-33 deletion in macrophages is not as simple as the shift from the M1 to M2 phenotype reported previously.[19] Thus, to establish that the silencing of miRNA is a therapeutic strategy for the treatment of humans, further detailed experiments are required.

Methods

Cell Culture and Reagents

Peritoneal macrophages were obtained from the peritoneal cavity of mice 4 days after intraperitoneal injection of 3 mL of 3% thioglycollate. For the analysis of M1/M2 markers, residual peritoneal macrophages were obtained without thioglycollate injection. The cells obtained were washed, spun at 1000 rpm for 5 minutes, and plated at a density of 5×10^5 cells/mL with RPMI1640 medium (Nacalai Tesque, Japan) containing 10% fetal bovine serum (FBS). J774 mouse macrophages were obtained from the American Type Cell Collection (Rockville, MD) and cultured with RPMI1640 medium containing 10% FBS. The antibodies used were an anti-ABCA1 antibody (NB400-105), an anti-ABCG1 antibody (NB400-132; Novus Biologicals, Littleton, CO), an anti-GAPDH antibody (#2118S), an anti-AMPKα antibody (#2532), an anti-cleaved-caspase-3 antibody (#9661S; Cell Signaling Technology, Beverly, MA), an anti-β-actin antibody (AC-15; A5441, Sigma-Aldrich, St. Louis, MO), an anti-RIP140 antibody (sc-8997), an anti-CD3ε antibody (sc-1127; Santa Cruz, Biotechnology, CA), an anti-αSMA antibody (MO0851, Dako, Glostrup, Denmark), an anti-CROT antibody (ab103448), an anti-CPT1A antibody (ab128568), an anti-iNOS antibody (ab3523), an anti-VCAM1 antibody (ab27560), an anti-ICAM1 antibody (ab25375), an anti-IL6 antibody (ab6672), an anti-IL10 antibody (ab33471; Abcam, Cambridge, UK), an anti-single-stranded DNA (ssDNA) antibody (No. 18731; IBL, Gunma, Japan), and an anti-CD68 antibody (FA-11; Serotec, Kidlington, UK). Human acetylated LDL (acLDL) and human HDL-C were purchased from Biomedical Technologies Inc (Stoughton, MA). Anti-rabbit and anti-mouse IgG HRP-linked antibody was purchased from GE Healthcare (Amersham, UK). Human apoA-I, polyethylene glycol (PEG), ACAT inhibitor, Cpt-cAMP, Sudan IV, and oil red O were from Sigma-Aldrich. [1, 2-^{3}H (N)]-Cholesterol was from Perkin Elmer (Boston, MA).

Generation of MiR-33 and ApoE Double-Knockout Mice

To obtain miR-33 and apoE double-knockout mice (miR-33$^{-/-}$ *Apoe*$^{-/-}$), miR-33$^{-/-}$ mice were mated with *Apoe*$^{-/-}$ mice, which were backcrossed to C57BL/6 mice for 10 generations.[20–22] Because both knockout mice had a BL/6 background,

miR-33$^{-/-}$*Apoe*$^{-/-}$ mice also had a BL/6 background. MiR-33$^{+/+}$*Apoe*$^{-/-}$ littermates were used as controls. After being weaned at 4 weeks of age, mice were fed normal chow (NC) containing 4.5% fat (Oriental Yeast, Tokyo, Japan) until 6 weeks of age and then switched to a Western-type diet (WTD) containing 0.15% cholesterol and 20% fat (Oriental Yeast) for 16 weeks. All the experimental protocols were approved by the Ethics Committee for Animal Experiments of Kyoto University.

Serum Lipid Profiling

After mice were fasted for 4 to 6 hours, blood was obtained from the inferior vena cava of anesthetized mice, and serum was separated by centrifugation at 4°C and stored at −80°C. Serum lipoproteins were measured by standard methods (Accelerator selective detergent method using a Hitachi 7180 Auto Analyzer; Nagahama Life Science Laboratory, Nagahama, Japan) and HPLC methods (Sky Light Biotech, Akita, Japan).

Western Blotting

Western blotting was performed using standard procedures as described previously.[23] A total of 20 μg of protein was fractionated using NuPAGE 4% to 12% Bis-Tris gels (Invitrogen) and transferred to a Protran nitrocellulose transfer membrane (Whatman). The membrane was blocked using 1× phosphate-buffered saline (PBS) containing 5% nonfat milk for 1 hour and incubated with the primary antibody (anti-ABCA1, 1:1000; anti-ABCG1, 1:1000; anti–cleaved caspase-3, 1:500; anti-AMPKα, 1:1000; anti-CROT, 1:100; anti-CPT1a, 1:1000; anti-RIP140, 1:500; anti-β-actin, 1:3000; anti-GAPDH, 1:3000) overnight at 4°C. Following a washing step in PBS-0.05% Tween 20 (0.05% T-PBS), the membrane was incubated with the secondary antibody (anti-rabbit or anti-mouse IgG HRP-linked, 1:2000) for 1 hour at 4°C. The membrane was then washed in 0.05% T-PBS and detected by ECL Western Blotting Detection Reagent (GE Healthcare) using an LAS-1000 system (Fuji Film).

RNA Extraction and Quantitative Real-Time PCR (qRT-PCR)

Total RNA was isolated and purified using TRIzol reagent (Invitrogen), and cDNA was synthesized from 1 μg of total RNA using Transcriptor First Strand cDNA Synthesis Kit (Roche) in accordance with the manufacturer's instructions. For qRT-PCR, specific genes were amplified by 40 cycles using SYBR Green PCR Master Mix (Applied Biosystems). Expression was normalized to the housekeeping gene *Actb*. Gene-specific primers are summarized as follows:

Il6 sense, 5′ ACCACGGCCTTCCCTACTTC 3′;
Il6 antisense, 5′ AGATTGTTTTCTGCAAGTGCATCA 3′;
Tnf sense, 5′ CCAGACCCTCACACTCAGATC 3′;
Tnf antisense, 5′ CACTTGGTGGTTTGCTACGAC 3′;
Nos2 (Inos) sense, 5′ GAGTCTTGGTGAAAGTGGTGTTC 3′;
Nos2 (Inos) antisense, 5′ TTCCCTGTCTCAGTAGCAAAGAG 3′;
Mmp2 sense, 5′ ATCTTTGCAGGAGACAAGTTCTG 3′;
Mmp2 antisense, 5′ TTCAGGTAATAAGCACCCTTGAA 3′;
Serpine 1 (Pai1) sense, 5′ TCAGCCCTTGCTTGCCTCAT 3′;
Serpine1 (Pai1) antisense, 5′ GCATAGCCAGCACCGAGGA 3′
Il10 sense, 5′ AAATAAGAGCAAGGCAGTGGAG 3′;
Il10 antisense, 5′ TCATTCATGGCCTTGTAGACAC 3′;
Arg1 sense, 5′ AACTCTTGGGAAGACAGCAGAG 3′;
Arg1 antisense, 5′ GTAGTCAGTCCCTGGCTTATGG 3′;
Retnla (*Fizz1*) sense, 5′ AGGATGCCAACTTTGAATAGGA 3′;
Retnla (*Fizz1*) antisense, 5′ AGTTAGCTGGATTGGCAAGAAG 3′;
Chi3l3 (*Ym-1*) sense, 5′ CCCACCAGGAAAGTACACAGA 3′;
Chi3l3 (*Ym-1*) antisense, 5′ CTCAGTGGCTCCTTCATTCAG 3′;
Emr1 (F4/80) sense, 5′ TCCAGAAGGCTCCCAAGGATA 3′;
Emr1 (F4/80) antisense, 5′ GGGCACTTTTGTTCTCACAGGTA 3′;
Abca1 sense, 5′ AACAGTTTGTGGCCCTTTTG 3′;
Abca1 antisense, 5′ AGTTCCAGGCTGGGGTACTT 3′;
Abcg1 sense, 5′ CTGCCTCACCTCACTGTTCA 3′;
Abcg1 antisense, 5′ TCTCGTCTGCCTTCATCCTT 3′;
Crot sense, 5′ TACTTTTACCACGGCCGAAC 3′;
Crot antisense, 5′ GACGGTCAAATCCTTTTCCA 3′;
Cpt1a sense, 5′ GATCTACAATTCCCCTCTGCTCT 3′;
Cpt1a antisense, 5′ TAGAGCCAGACCTTGAAGTAACG 3′;
Prkaa1 (*AMPKα1*) sense, 5′ AGAGGGCCGCAATAAAAGAT 3′
Prkaa1 (*AMPKα1*) antisense, 5′ TGTTGTACAGGCAGCTGAGG 3′;
Nrip1 (*RIP140*) sense, 5′ AGCAGGACAAGAGTCACAGAAAC 3′;
Nrip1 (*RIP140*) antisense, 5′ TGTGATGATTGGCAGTATCTACG 3′;
Actb sense, 5′ GATCTGGCACCACACCTTCT 3′;
Actb antisense, 5′ GGGGTGTTGAAGGTCTCAAA 3′;

Quantitative PCR for MicroRNA

Total RNA was isolated using TRIzol reagent (Invitrogen). MiR-33 was measured in accordance with the TaqMan MicroRNA Assays (Applied Biosystems) protocol, and the products were analyzed using a thermal cycler (ABI Prism7900HT sequence detection system). Samples were normalized by U6 snRNA expression.

Cholesterol Efflux via Mouse ApoB-Depleted Serum

Cholesterol efflux via mouse apoB-depleted serum was measured as described previously.[24,25] Briefly, J774 cells were plated in 24 multiwell plates (7×10^4 cells/well) and labeled for 24 hours using ^{3}H-cholesterol (2 μCi/mL) in RPMI1640 plus 1% FBS. Cells were incubated in RPMI1640 containing Cpt-cAMP (0.3 mmol/L) and 0.2% BSA for an additional 16 hours to upregulate ABCA1 in J774 cells. Cells were washed and incubated for 4 hours in MEM-HEPES

containing 2.8% apoB-depleted serum (equivalent to 2% serum), which was obtained after apoB lipoproteins were removed with PEG.[26] All steps were performed in the presence of acyl-coenzyme A:cholesterol acyltransferase (ACAT) inhibitor (2 μg/mL). Cholesterol efflux was expressed as the percentage of radioactivity released from the cells in the medium relative to the total radioactivity in cells plus medium.

Cholesterol Efflux From Mouse Peritoneal Macrophages

Cellular cholesterol efflux via apoA-I and HDL was determined as described previously.[22,27] Briefly, thioglycollate-elicited mouse peritoneal macrophages were plated in 24-well multiplates at a density of 5×10^6 cell/mL. Cells were cultured for 24 hours in RPMI1640 containing ^{3}H-labeled acLDL (1.0 μCi/mL of ^{3}H-cholesterol and 25 μg/mL of acLDL). On the next day, cells were washed 3 times with RPMI1640, then incubated for 6 hours in RPMI1640 with or without apoA-I or HDL as indicated concentrations. Cholesterol efflux was expressed as a percentage of the radioactivity released from cells in medium relative to the total radioactivity in cells plus medium.

Flow Cytometry

Peripheral blood was collected from the orbital sinuses of 12-week-old miR-33$^{+/+}$*Apoe*$^{-/-}$ and miR-33$^{-/-}$*Apoe*$^{-/-}$ mice that were given an NC diet using heparin-coated capillary tubes. Total leukocytes were quantified from whole blood using a hematology cell counter (Celltac α MEK-6358, Nihon Kohden). Erythrocytes were lysed using a commercial RBC lysis solution (BD PharmLyse, BD Biosciences). Monocytes were identified by staining with anti-CD115–Alexa Fluor 488 antibody (eBioscience clone AFS98), and monocyte subsets were identified by staining with anti-Ly6C-APC antibody (eBioscience, clone HK1.4). Data were acquired using a BD FACSaria Flow Cytometer and analyzed with BD FACSDiva software (BD Biosciences).

Bone Marrow Transplantation (BMT) and Assessment of Chimerism

Male mice with genotypes of miR-33$^{+/+}$*Apoe*$^{-/-}$ and miR33$^{-/-}$*Apoe*$^{-/-}$ (8 weeks old) were used as bone marrow (BM) donors. BM recipients were female miR-33$^{+/+}$*Apoe*$^{-/-}$ mice and miR-33$^{-/-}$*Apoe*$^{-/-}$ mice (8 weeks old). Thus, all the experimental mice used for BM transplantation (BMT) had an *Apoe*$^{-/-}$ background. BM donors were euthanized by cervical dislocation, and BM cells were collected by flushing femurs and tibias with PBS supplemented with 3% FBS. The suspension was passed through 40-μm nylon mesh (Cell Strainer, BD Biosciences). Red blood cells were lysed using ACK lysing buffer (Lonza). BM cells were then washed twice with PBS supplemented with 3% FBS. To induce BM aplasia, recipients were irradiated with 2 doses of 6 Gy within an interval of 3 hours (cesium 137; Gammacell 40 Exactor) and injected intravenously with 5×10^6 BM cells 6 hours after irradiation.[28,29] After BMT, mice were fed NC diet for 4 weeks and then switched to a WTD for 12 weeks. At age 24 weeks, mice were euthanized and analyzed. The hematologic chimerism of mice was determined by PCR using genomic DNA from blood, BM, and tail with the PCR primers described above and by measuring miR-33 levels in BM cells by quantitative PCR at age 24 weeks (ie, 16 weeks after BMT).

Quantification of Atherosclerosis

Atherosclerotic lesions were quantified by en face analysis of the whole aorta and by cross-sectional analysis of the proximal aorta.[30–32] For the en face analysis of the aorta, the Sudan IV-stained aortas were photographed and used for the quantification of atherosclerotic lesions. The total aortic surface area and the lesion area were measured by image analysis (ImageJ), and the ratio of the lesion area to the total area was calculated. For the cross-sectional analysis of the aorta, the OCT-embedded aortas were sectioned using a cryostat, and 6-μm sections were obtained sequentially beginning at the aortic valve. Eight sections obtained every 24 μm from the aortic sinus were stained with oil red O and used for the quantification of lesion areas. The lesion areas of each aorta were measured using ImageJ. The average of the 8 sections from 1 mouse was taken as a value that represented the mouse.

Immunohistochemistry

Eight sections of aortic root per mouse were stained with an anti-CD68 antibody (1:200), anti-CD3 antibody (1:50), anti-α smooth muscle actin (SMA) antibody (1:50), anti-ssDNA antibody (1:600), anti-iNOS antibody (1:200), anti-VCAM-1 antibody (1:50), anti-ICAM-1 antibody (1:50), anti-IL-6 antibody (1:400), and anti-IL-10 antibody (1:50). The lesion and positively stained areas of each aorta were measured using ImageJ. The average of the 8 sections from 1 mouse was taken as a value that represented the mouse.

Apoptosis Assay

After being washed 3 times in PBS, peritoneal macrophages were loaded with free cholesterol (FC) by incubation with RPMI1640 containing 10% FBS supplemented with or without 300 μg/mL of acLDL plus 10 μg/mL of ACAT inhibitor (58035). The next day, cells were assayed for early- to midstage

apoptosis by staining with Alexa Fluor 488–conjugated annexin V (green), as described previously[27,33,34], using a Vybrant Apoptosis Assay Kit (Molecular Probes). Representative fields (4 to 6 fields containing ≈1000 cells) were photographed. The number of annexin V–positive cells was counted and expressed as a percentage of the total number of cells in at least 4 separate fields. For Western blotting of cleaved caspase-3, the samples were collected 48 hours after stimulation.

Measurement of Serum ApoA-I Levels

We quantified serum apoA-I levels in mice using an ELISA assay kit for mouse apoA-I in accordance with the manufacturer's instructions (USCN Life Science Inc, Wuhan, China).

Measurement of Total Cholesterol, Free Cholesterol, Cholesterol Ester, and Triglyceride in the Liver

Lipids in the liver were extracted by the Folch procedure[35] and quantified using standard enzymatic colorimetric methods.

Statistics

Data are presented as mean±SE. Statistical comparisons were performed using nonparametric analysis when the group numbers were <10 (Mann–Whitney *U* test). Otherwise, unpaired 2-tailed Student *t* tests were conducted. Statistical significance was tested by a 1-way analysis of variance with the Bonferroni post hoc test when experiments included >2 groups. The level of significance was set at a probability value of <0.05.

Results

MiR-33 Deficiency Reduced Atherosclerosis

To clarify the role of miR-33 in the progression of atherosclerosis, miR-33$^{-/-}$ mice[22] were mated with *Apoe*$^{-/-}$ mice.[20,21] Because both lines have a BL/6 background, miR-33$^{-/-}$*Apoe*$^{-/-}$ double-knockout mice also had a BL/6 background. The miR-33$^{-/-}$*Apoe*$^{-/-}$ mice were born at the expected Mendelian ratio, and miR-33$^{+/+}$*Apoe*$^{-/-}$ littermates were used as controls. The miR-33$^{+/+}$*Apoe*$^{-/-}$ and miR-33$^{-/-}$*Apoe*$^{-/-}$ mice were fed a WTD containing 0.15% cholesterol

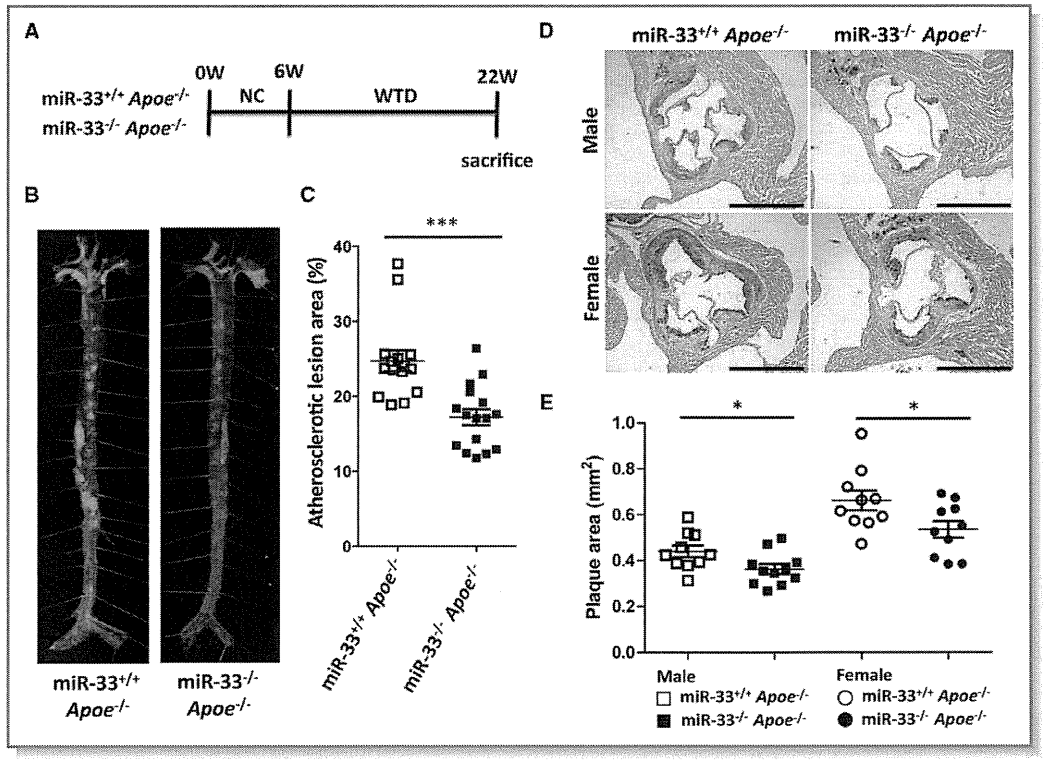

Figure 1. miR-33 deficiency reduced atherosclerosis. A, Experimental protocol for the analysis of atherosclerosis in miR-33$^{+/+}$*Apoe*$^{-/-}$ and miR-33$^{-/-}$*Apoe*$^{-/-}$ mice. B, Representative images of the en face analysis of the total aorta in miR-33$^{+/+}$*Apoe*$^{-/-}$ and miR-33$^{-/-}$*Apoe*$^{-/-}$ male mice. C, Quantification of the atherosclerotic lesion area in en face analysis of the total aorta in male mice. Values are mean±SE (n=15 to 16 each); ***P<0.001. D, Representative microscopic images of cross-sections of proximal aorta in miR-33$^{+/+}$*Apoe*$^{-/-}$ and miR-33$^{-/-}$*Apoe*$^{-/-}$ male and female mice. Scale bar: 1 mm. E, Quantification of the atherosclerotic plaque area in cross-sections of proximal aorta in male and female mice. Values are mean±SE (n=10 to 11 each); *P<0.05.

beginning at age 6 weeks, and atherosclerotic lesions were analyzed at age 22 weeks (Figure 1A). The atherosclerotic lesion area was examined by an èn face analysis of the total aorta and cross-sections of the proximal aorta. The en face analysis of the total aorta showed that atherosclerotic lesions throughout the aorta were significantly reduced in miR-33$^{-/-}$ *Apoe*$^{-/-}$ mice compared with miR-33$^{+/+}$ *Apoe*$^{-/-}$mice (male: P<0.001, 24.7±1.4% versus 17.2±1.1%, Figure 1B and 1C). The plaque area in the proximal aorta was extensively examined in males and females. Atherosclerotic lesions were significantly reduced in miR-33$^{-/-}$*Apoe*$^{-/-}$ mice of both sexes (male: P=0.0314, 0.44±0.025 versus 0.36±0.021 mm^2; female: P=0.0372, 0.66±0.042 versus 0.54 ± 0.036 mm^2; Figure 1D and 1E). The plaque area in females was greater than that in males. Moreover, the quantification of lipid accumulation by oil red O staining showed a significant decrease in miR-33$^{-/-}$*Apoe*$^{-/-}$ compared with miR-33$^{+/+}$ *Apoe*$^{-/-}$ mice (P=0.034, 9.8±1.1% versus 7.1±0.5%; Figure 2A and 2B). To further analyze lesion macrophages in these mice, we stained aortic plaque using an anti-CD68 antibody. The CD68-positive area was also significantly decreased in the proximal aortas of miR-33$^{-/-}$*Apoe*$^{-/-}$ mice compared with miR-33$^{+/+}$*Apoe*$^{-/-}$ mice (P=0.0022, 24.9±1.0% versus 20.5±0.7%; Figure 2C and 2D). We also analyzed CD3-positive cells, αSMA-positive area, and picrosirius red staining for collagens (Figure 3A through 3F). CD3-positive cells were significantly reduced in miR-33$^{-/-}$*Apoe*$^{-/-}$

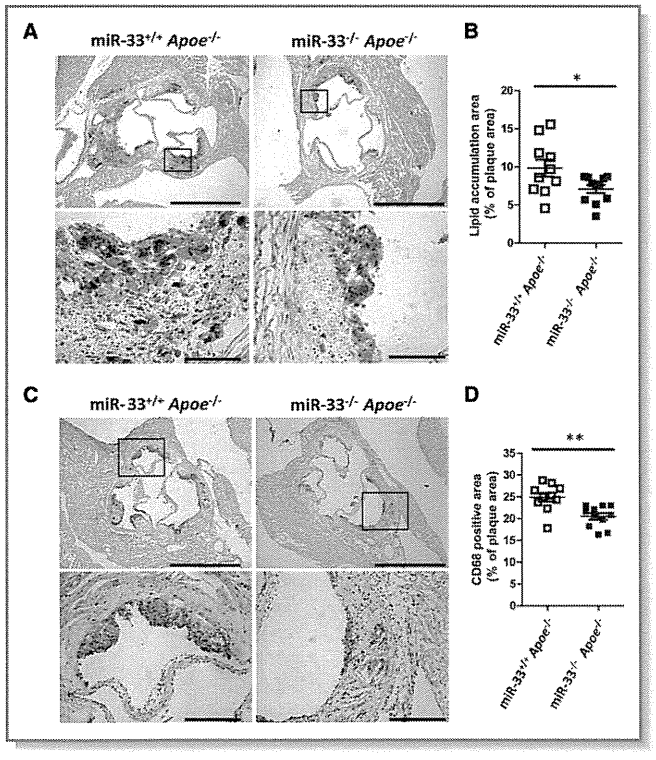

Figure 2. miR-33 deficiency reduced lipid accumulation and macrophage content in atherosclerotic plaque. A, Representative microscopic images of the lipid accumulation area in cross-sections of proximal aorta in miR-33$^{+/+}$*Apoe*$^{-/-}$ and miR-33$^{-/-}$*Apoe*$^{-/-}$ male mice. Scale bars: 1 mm (upper), 100 μm (lower). B, Quantification of lipid accumulation area in cross-sections of proximal aorta in male mice. Values are mean±SE (n=10 to 11 each); *P<0.05. C, Representative microscopic images of immunohistochemical staining for the macrophage marker CD68 in male mice. Scale bars: 1 mm (upper), 200 μm (lower). D, Quantification of the CD68-positive area in cross-sections of proximal aorta in male mice. Values are mean±SE (n=10 to 11 each); **P<0.01.

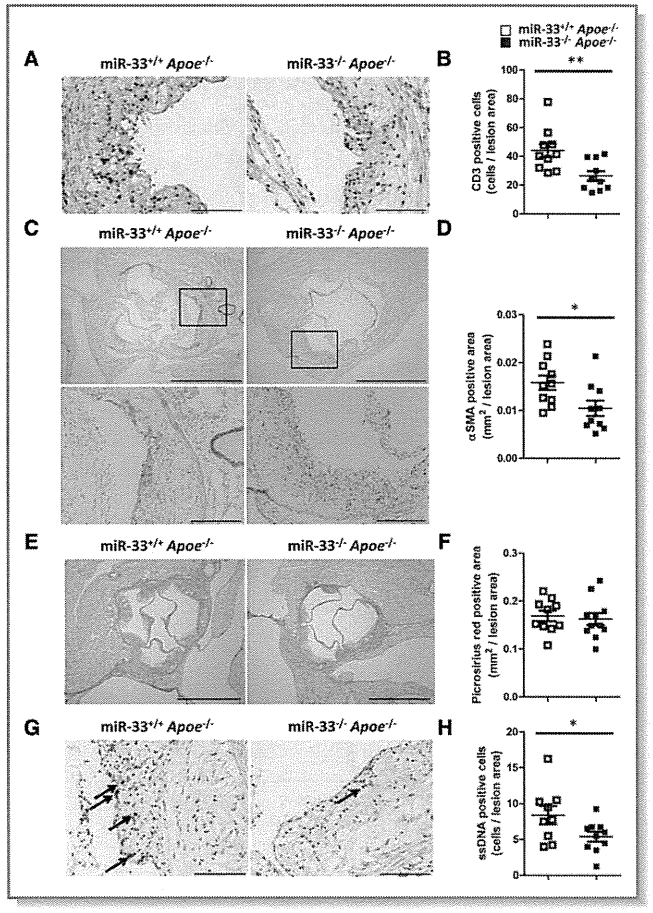

Figure 3. miR-33 deficiency reduced CD3-positive cell accumulation and apoptosis in atherosclerotic plaque. A, Representative microscopic images of immunohistochemical staining for the T-cell marker CD3 in male mice. Scale bar: 100 μm. B, Quantification of CD3-positive cells in cross-sections of proximal aorta in male mice. Values are mean±SE (n=10 each); **P<0.01. C, Representative microscopic images of immunohistochemical staining for αSMA in male mice. Scale bars: 1 mm (upper), 200 μm (lower). D, Quantification of the αSMA-positive area in cross-sections of proximal aorta in male mice. Values are mean±SE (n=10 each); *P<0.05. E, Representative microscopic images of picrosirius red staining for the collagen in male mice. Scale bar: 1 mm. F, Quantification of the picrosirius red–positive area in cross-sections of proximal aorta in male mice. Values are mean±SE (n=10 to 11 each). G, Representative microscopic images of immunohistochemical staining for ssDNA in male mice. Scale bar: 100 μm. H, Quantification of ssDNA-positive cells in cross-sections of proximal aorta in male mice. Values are mean±SE (n=9 to 10 each); *P<0.05.